This article was downloaded by:
On: *26 January 2011*
Access details: *Access Details: Free Access*
Publisher *Taylor & Francis*
Informa Ltd Registered in England and Wales Registered Number: 1072954 Registered office: Mortimer House, 37-41 Mortimer Street, London W1T 3JH, UK

Liquid Crystals
Publication details, including instructions for authors and subscription information:
http://www.informaworld.com/smpp/title~content=t713926090

Strongly non-linear optical ferroelectric liquid crystals for frequency doubling

K. Schmitt[a]; R. -P. Herr[a]; M. Schadt[a]; J. Fünfschilling[a]; R. Buchecker[a]; X. H. Chen[b]; C. Benecke[a]
[a] Dept. RLCR, F. Hoffman-La Roche Inc., Basel, Switzerland [b] Technical University of Berlin, Berlin, Germany

To cite this Article Schmitt, K. , Herr, R. -P. , Schadt, M. , Fünfschilling, J. , Buchecker, R. , Chen, X. H. and Benecke, C.(1993) 'Strongly non-linear optical ferroelectric liquid crystals for frequency doubling', Liquid Crystals, 14: 6, 1735 — 1752
To link to this Article: DOI: 10.1080/02678299308027712
URL: http://dx.doi.org/10.1080/02678299308027712

PLEASE SCROLL DOWN FOR ARTICLE

Full terms and conditions of use: http://www.informaworld.com/terms-and-conditions-of-access.pdf

This article may be used for research, teaching and private study purposes. Any substantial or systematic reproduction, re-distribution, re-selling, loan or sub-licensing, systematic supply or distribution in any form to anyone is expressly forbidden.

The publisher does not give any warranty express or implied or make any representation that the contents will be complete or accurate or up to date. The accuracy of any instructions, formulae and drug doses should be independently verified with primary sources. The publisher shall not be liable for any loss, actions, claims, proceedings, demand or costs or damages whatsoever or howsoever caused arising directly or indirectly in connection with or arising out of the use of this material.

LIQUID CRYSTALS, 1993, VOL. 14, NO. 6, 1735–1752

Strongly non-linear optical ferroelectric liquid crystals for frequency doubling

by K. SCHMITT*, R.-P. HERR, M. SCHADT, J. FÜNFSCHILLING, R. BUCHECKER, X. H. CHEN† and C. BENECKE

F. Hoffman-La Roche Inc.,
Dept. RLCR, 4002 Basel,
Switzerland
†Technical University of Berlin,
Inst. Organic Chemistry (3)
1000 Berlin 12, Germany

From our research for novel non-linear optical (NLO) materials for frequency doublers and optical modulators we report on new ferroelectric liquid crystals, which for the first time, exhibit second order NLO coefficients (for example $d_{22} = 5\,\text{pm V}^{-1}$, which are comparable to those of state of the art inorganic NLO materials. The novel compounds contain 5-amino-2-nitrophenyl groups attached close to the chiral centres. The switching behaviour of the new compounds, their spontaneous polarization, as well as their frequency doubling of Nd:YAG laser pulses in the S_C^* and in the glass state, are reported. Moreover their waveguiding properties are presented.

Downloaded At: 11:08 26 January 2011

1. Introduction

Since the early days of ferroelectric liquid crystal (FLC) research, exploration of the non-linear optical properties of these substances has been a topic of interest [1–3]. The S_C^* phase and other chiral tilted phases are non-centrosymmetric and therefore may exhibit second order non-linear (NLO) responses. This includes effects like second harmonic generation (SHG) and the Pockels effect, to name those most frequently investigated. However, until recently the reported NLO efficiencies of FLCs [4, 5] have turned out to be so small that these materials seemed to be irrelevant for any NLO device application.

The main reason for the low electronic NLO activity is that the FLC compounds and mixtures used in these investigations were optimized for display applications rather than for NLO performance. Fairly recently some research groups [6, 7] started developing FLC compounds specifically devoted to NLO applications, and indeed improved the SHG efficiency by orders of magnitude [8]. But still the highest reported values of the NLO coefficients d_{ij}, being in the order of 0·1 to 0·6 pm V^{-1}, were too small to be competitive with state of the art NLO materials such as $LiNbO_3$ or poled NLO polymers.

In this paper we present new FLC materials (see tables 1 (*a*) and (*b*)) that exhibit coefficients which are nearly one order of magnitude larger than those reported so far. Furthermore, some of our compounds and mixtures show a glass transition above room temperature which allows us to freeze the NLO active orientation, thus

* Author for correspondence.

0267–8292/93 $10·00 © 1993 Taylor & Francis Ltd.

leading to stable SHG active orientations. Moreover, we demonstrate the waveguiding capability of these new materials, which renders them particularly interesting in the field of integrated optics.

2. Design considerations

In order to create FLC materials with improved second order NLO activity one might consider implanting well known NLO chromophores into the core of standard FLC molecules. However, since the direction of dipolar orientation of the FLC molecules is parallel to the C_2 axis (perpendicular to the director) these NLO active molecular groups have to be incorporated in such a fashion that the direction of maximum second order polarizability is polarly oriented along this axis. This is expected to occur if the chromophore is coupled to the chiral centre of the molecule, because the specific nature of the chiral group defines the tilt direction and hence the direction of the polar axis. This requirement is automatically fulfilled if the chirality is part of the NLO group. If this is not the case, it seems to be advantageous to locate the two groups as close to each other as possible.

NLO chromopores with large β values normally consist of a donor and an acceptor group which are linked by a conjugated spacer, often in the form of aromatic rings. The direction of large second order polarizability is then roughly along the donor-acceptor axis; 4-nitroaniline and dimethylamino-nitrostilbene are classical examples [9]. In view of the symmetry requirements discussed above, such NLO chromophores have to be integrated in the FLC structure with their long axis perpendicular to the long axis of the liquid crystal molecule. It follows that the FLC molecular structure, being of a rod-like shape, can only then be compatible with such a functionalization if the NLO group is sufficiently compact and the rigid core of the LC molecule sufficiently long.

Considering these conditions, it is tempting to choose 4-nitroaniline moieties as promising functional NLO groups, in particular because the aromatic linking ring is a constituent of most FLC cores.

This concept has also been tested by other researchers [10], but to our knowledge it has not yet been demonstrated that 4-nitroaniline derivatives are compatible with mesogenic molecular structures, let alone with molecules exhibiting S_C^* phases. Of course, non-mesogenic chiral molecules can also be dipolarly oriented in S_C host matrices, but this means dilution, and hence a reduction in the NLO efficiency of the material. It is, therefore, highly desirable to create molecules that combine chirality, NLO activity, and S_C^* mesomorphic properties.

We will show that this concept indeed works for certain, specially designed structures.

3. Experimental

The synthesis of the new FLCs will be published separately.

DSC measurements were carried out at various heating and cooling rates using a Perkin–Elmer DSC 7. The data analysis was performed by means of the Perkin–Elmer software package TAS. The spontaneous polarization as a function of temperature was measured applying the usual triangular voltage method, where the frequency (10 Hz to 0·001 Hz) was appropriately adjusted to be compatible with the strongly temperature dependent viscosity of the materials. At higher temperatures, the observed signal included a considerable ohmic contribution due to ionic impurities. Electro-optical switching and tilt angle measurements, as well as LC texture observations, were performed using polarizing microscopes.

Downloaded At: 11:08 26 January 2011

The samples were temperature controlled in a Mettler FP2 heating stage or in special stages of our own design. The temperature stability was better then 0·5°C.

Homogeneously aligned cells of 1·9 to 7 μm thickness were prepared by filling prefabricated test cells by capillary action at temperatures around T_c; the glass walls were ITO coated and covered with a rubbed polyimide layer.

10 to 20 μm thick, homeotropically aligning FLC cells were made using metal spacers (aluminium) as electrodes which generate an electric field in the plane of the cell. The electrode gap was between 200 and 500 μm. Before filling with the FLC material, the cells were flushed with an orienting agent that favours homeotropic alignment (Merck Liquicoat). Thin homeotropically aligned cells (2 μm thick) were prepared by sputtering two aluminium electrodes (gap = 200 μm) on to the surface of one of the glass substrates and then spinning on a thin layer of Liquicoat. In this case the FLC alignment was further improved by shearing the cell in the S_A phase. After cooling to room temperature, the cell was sealed by an epoxy adhesive.

A third type of homeotropically aligned cell was used in the waveguiding studies. In this case, one of the substrates was a specially prepared high index glass prism (SF10). As schematically shown in figure 1 one-half of the prism surface at the substrate–liquid crystal interface was coated with a thin (200 nm) quartz layer, such that a sudden index jump from $n(\text{SF10}) = 1{\cdot}73$, in the uncoated area to $n(\text{quartz}) = 1{\cdot}46$, within the quartz coated area was produced. This allowed us to couple light beams of s and p polarization into the FLC layers using HeNe lasers at $\lambda = 1152$ nm, 633 nm and 543 nm, as well as an Ar ion laser at 488 nm.

The determination of the refractive indices, anisotropy and dispersion of the FLC materials was performed by analysing the mode spectra of TE and TM modes at various wavelengths. The temperature dependence of the ordinary index of refraction n_0 was measured by means of a modified Abbé refractometer (Atago T2). In this case a homeotropically aligned FLC layer on top of the refractometer prism was covered with a high index glass plate ($n = 1{\cdot}83$), which was illuminated from the front with monochromatic light in the range between 500 and 650 nm. Polarized observation allows one to detect the n_0 component.

Waveguiding experiments were performed by turning the prism cells on a rotating stage and measuring the guided light intensity *via* the light scattered by the waveguide with a photodiode (see figure 1).

The damping factors of the guided modes were determined *via* the intensity decay of the scattered light along the streak. In this case a particular mode was selected; by choosing the appropriate polarization and angle of incidence and then moving a slit aperture (100 μm width) along the streak by a translation stage, the intensity was measured by a photodiode behind the aperture.

The SHG experiments were performed using the apparatus schematically shown in figure 2. The second harmonic power $p^{2\omega}$ was measured in transmission as a function of the angle of incidence, polarization, temperature and applied external DC and AC electric field. In the case of the AC excitation of the sample, the laser was synchronized with respect to the phase of the applied AC voltage via a trigger delay generator. The laser source was a Q switched Nd : YAG laser (Spectra Physics DCR-11) producing 9 ns wide, 1064 nm pulses at a maximum repetition rate of 10 Hz. The pulses were attenuated to between 10 and 100 μJ. The signal was detected by a photomultiplier after passing a combination of an IR blocking filter and a 532 nm interference filter. The signal trace was stored on a storage oscilloscope (Tektronix 2232) and then transferred to a microcomputer for further processing.

Downloaded At: 11:08 26 January 2011

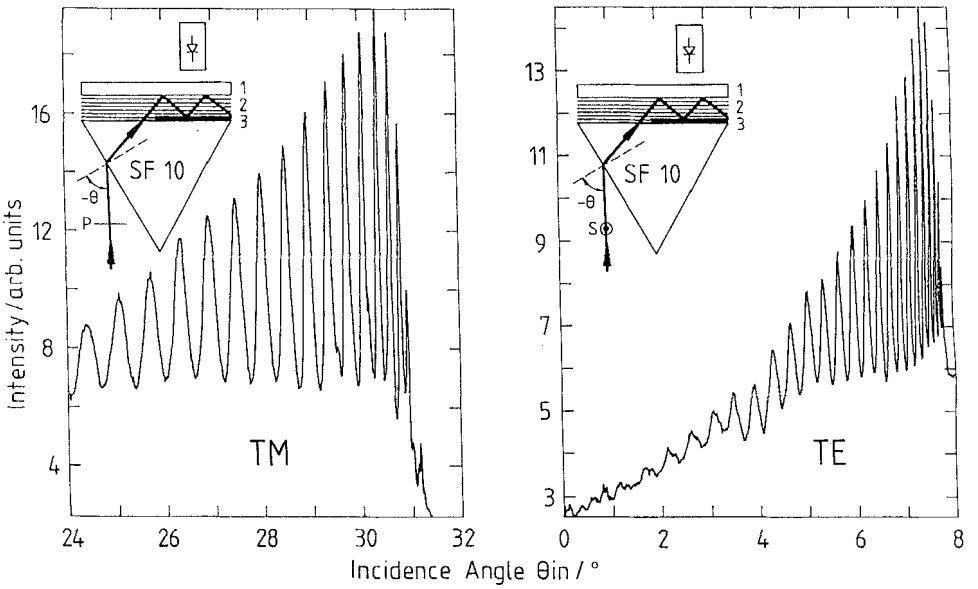

Figure 1. TE and TM mode spectra generated using a 12 μm thick containg a homeotropically aligned FLC layer of mixture **7**/**8**. The inserts show the overall layout of the prism cell; 1 and 3 are quartz layers, 2 is the FLC layer.

Downloaded At: 11:08 26 January 2011

The absolute pulse energy of the fundamental beam was measured with a power meter (Gen Tec Ed-X) while the absolute intensity of the second harmonic signal was determined by comparison with the second harmonic signal created by a 1700 μm thick quartz crystal using the known value of the d_{11} component (0·4 pm V^{-1}) of quartz as a reference. The polarization of the fundamental beam was defined by the combination of a rotatable $\lambda/2$ plate and a high power Glan Tompson polarizer; a rotatable sheet analyser selected the polarization component of the

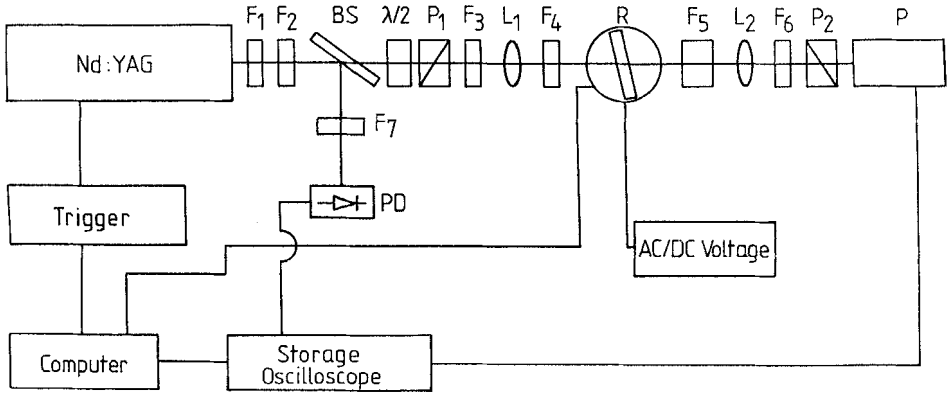

Figure 2. Schematic representation of the SHG experiments; F1 to F7 are filters, BS = beam splitter, $\lambda/2$ = halfwave plate, R = rotating stage, L1, L2 = lenses and PD = photodiode.

second harmonic pulse. An optional polarization microscope (not shown in figure 2) was used to inspect the LC cell *in situ* during the SHG experiment. This was helpful for checking the alignment quality of the cell under investigation.

Three cell geometries were used in this study. 1. For screening experiments, homogeneously aligned cells were used at an oblique angle of incidence (typically 45° incidence). 2. Phase matching properties were determined using homeotropically aligned cells which were angular tuned about the dipolar axis *Y* (see figure 3). Spectra using *p* as well as *s* polarized light were recorded. 3. For determining the d_{22} component of the NLO FLC materials, thin (2 μm) homeotropic cells were irradiated at normal incidence polarized along *Y*.

4. Results and discussion

4.1. *New NLO materials*

We first designed and synthesized the three-ring molecules shown in table 1 (*a*). None of these exhibits a mesophase; thus we investigated their NLO properties by using them as chiral dopants in our standard S_C host mixtures. Unfortunately, the solubility of these compounds is low, so that only concentrations up to 7 per cent by weight could be investigated. Table 1 (*a*) shows their spontaneous polarization P_s extrapolated to 100 per cent concentration. The resulting P_s values are fairly small; this indicates that the strong dipole moment of the 4-nitroaniline headgroup is only very slightly oriented along the C_2 axis of the S_C^* test mixture.

Based on our design concept, this could mean that a three-ring core is not long enough to compensate for the lateral extension caused by the NLO chromophore. Therefore we decided to extend the rigid cores to 4-ring systems. Moreover, we modified the NLO chromophores from 4-nitroaniline moieties to the corresponding biphenyl chromophores. Table 1 (*b*) shows four examples (compounds **4**, **6**, **7**, and **8**). All of them exhibit improved P_s values, and all, except compound **4**, exhibit mesophases; compounds **7** and **8** even show S_C^* phases.

Downloaded At: 11:08 26 January 2011

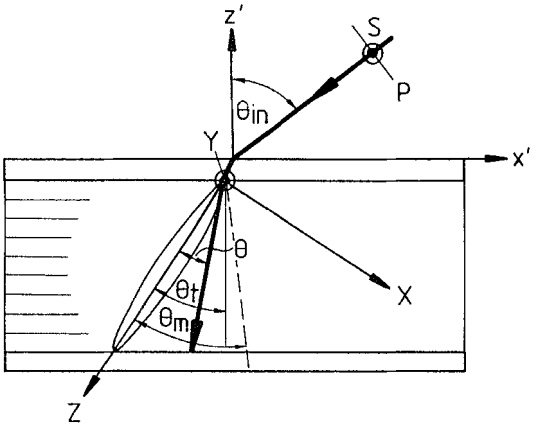

Figure 3. Schematic representation of the coordinate systems and angles used for the NLO experiments made using homeotropically aligned cells. θ_t is the tilt angle, θ_m the phase matching angle; s and p are the polarizations of the incident beam in the plane of incidence and normal to it.

Table 1. (*a*) Structure, melting temperatures, and induced spontaneous polarization P_s of new compounds containing single ring 4-nitroaniline moiety NLO chromophores. P_s of a S_C host mixture doped with 7 per cent of the NLO active compound is measured 15°C below the S_A–S_C^* transition extrapolated to 100 per cent concentration. (*b*) Structure, phase transition temperature and spontaneous polarization of the new compounds containing biphenyl-containing NLO chromophores. ( ) represents a monotropic transition temperature; ⊕ the P_s were measured using a S_C^* host mixture at 15°C below the S_A–S_C^* phase transition and extrapolation 100 per cent concentration; † the P_s were measured using the pure compound (100 per cent). The number of + signs in the final column is a qualitative measure of the SHG efficiency.

No.	Structure	mp/°C	P_s/nC cm^{-2}	SHG
1	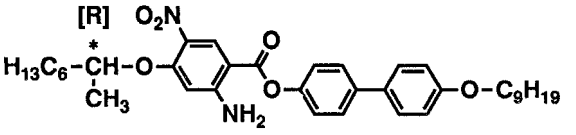	132.9–134.4	58	+
2	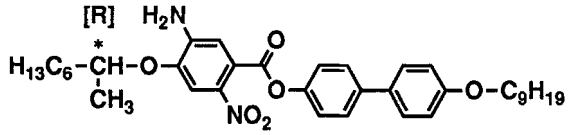	140.5–142.2	131	+
3	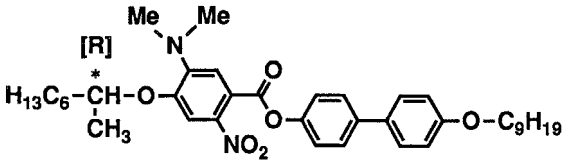	59.6–62.4	5	+

(*a*)

General structure: 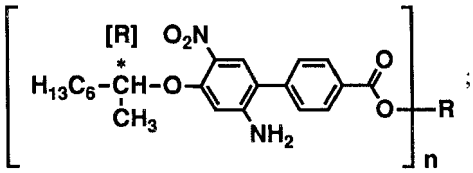 ; $n = 1,2$

No.	*n*	*R*	C–S_C^*/S_A/I	S_C^*–S_A	S_A–Ch/I	Ch/I	P_s/nC cm^{-2}	SHG
4	1	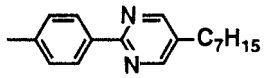	175–176.1				141⊕	+
5	1	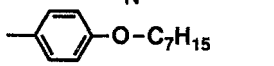	91		(74)		208⊕	+ + +
6	1	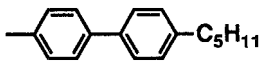	142		160.8	168.1	207†	+ +
7	1	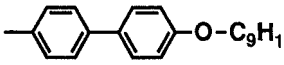	80	132	186		306†	+ + +
8	1	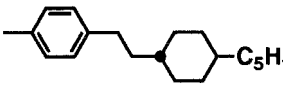	110	(62)	132	139	179⊕	+ + +
9	2	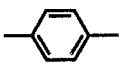	175		186	201	139⊕	+

(*b*)

Downloaded At: 11:08 26 January 2011

Compound **5** (table 1 (*b*)) shows interesting aspects: being a 3-ring compound, it exhibits only a monotropic S_A phase, but the dipolar alignment of the biphenyl chromophore along the C_2 axis is drastically improved as indicated by the large P_s value.

The five-ring compound **9** also depicted in table 1 (*b*), possesses chiral groups and the associated NLO chromophores at both ends of the rigid core. In this way, we tried to increase the chromophore concentration. As shown by the low P_s value, this attempt evidently failed.

Qualitative SHG measurements made with single components of the new compounds and with test mixtures gave results which correlate with the P_s data: as indicated by the number of + signs in the last row of tables 1 (*a*) and 1 (*b*), those compounds exhibiting large P_s values also show strong SHG responses. From these data it follows that compound **7** is the most promising candidate for an efficient SHG material. Due to its high viscosity, poor homogeneous aligning properties and high clearing temperature, this substance is however difficult to handle. Therefore we selected the two compounds **7** and **8** for further NLO investigations. These were made by using the single compound **7** and a 1 : 1 mixture of compounds **7** and **8** (mixture **7**/**8**).

Downloaded At: 11:08 26 January 2011

4.2. *Results for compound* **7**

4.2.1. *Phase assignment*

The DSC data for compound **7** reveal a strong melting peak at 80°C in the first heating run, a clearing transition at about 186°C, and two small peaks at about 132 and 96°C; the compound is easily supercooled and gives rise to a strong glass transition at around 35°C. These data are in agreement with the texture changes observed by polarizing microscopy. A typical fan-shaped texture (S_A phase) is observed above 132°C and changes to a broken fan texture (S_C^* phase) below this temperature. The texture changes slightly again below 96°C, indicating a further phase transition, probably to a higher ordered tilted phase (S_X). This S_X phase can be cooled down to room temperature without further texture changes.

4.2.2. *Tilt angle*

The temperature and electric field dependence of the tilt angle measured using a thin (2 μm), homogeneously oriented cell is shown in figure 4 (*a*). Due to the electroclinic effect, the switching angle is proportional to the electric field above the S_A–S_C^* transition. Far below the phase transition, it resembles that of typical S_C^* materials: above a threshold voltage, the switching angle is independent of the electric field and increases with decreasing temperature. Interestingly, there occurs an anomalous reduction in the switching angle around 90°C, probably caused by the S_C^*–S_X transition. Below this transition the angle increases again.

4.2.3. *Spontaneous polarization* P_s

The temperature dependence of P_s of compound **7** also exhibits the typical features of a FLC substance. At the S_A–S_C^* transition, the characteristic peak in the voltage dependence of the switching current appears and increases with decreasing temperatures. For P_s we determined 350 nC cm^{-2} at 120°C and 750 nC cm^{-2} at 50°C. Unfortunately, we could not follow the P_s to lower temperatures because, due to the rapidly increasing viscosity, switching was so slow (in the 100 s range at 50°C) and the current peak so broad that the triangular voltage method was no longer

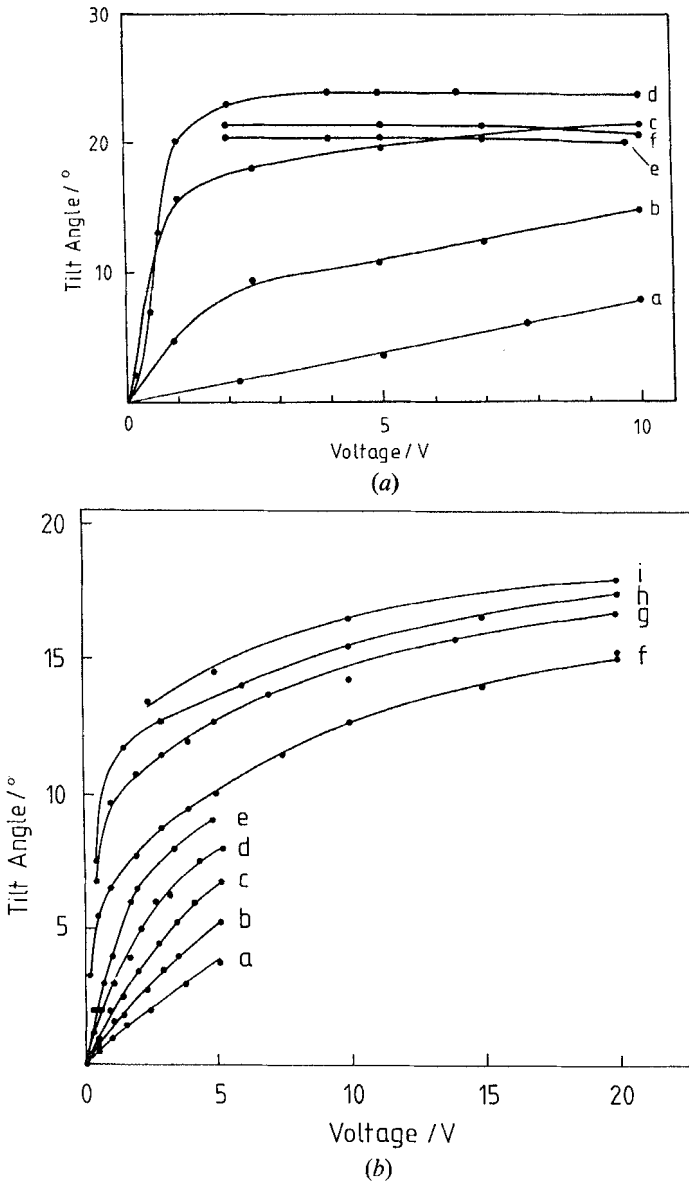

Figure 4. (*a*) Electric field dependence of the tilt angle θ_t of compound **7** at various temperatures; $a = 140°C$, $b = 133°C$, $c = 114°C$, $d = 100°C$, $e = 80°C$, and $f = 58°C$. (*b*) Electric field dependence of the tilt angle θ_t of mixture **7**/**8** at various temperatures; $a = 87°C$, $b = 76°C$, $c = 70°C$, $d = 65°C$, $e = 60°C$, $f = 55°C$, $g = 42°C$, $h = 38°C$, and $i = 33°C$.

applicable. We conclude: 1. the P_s of compound **7** is $> 750\,nC\,cm^{-2}$ at low temperatures, and 2. the S_X phase is also ferroelectric.

4.2.4. *SHG measurements*

The SHG signal (see figure 5), measured using a homeotropically aligned cell of 20 μm thickness (electrode gap 500 μm) at normal incidence, exhibits the characteristic features that have also been observed for other FLC systems [11, 12]. In the S_A

Downloaded At: 11:08 26 January 2011

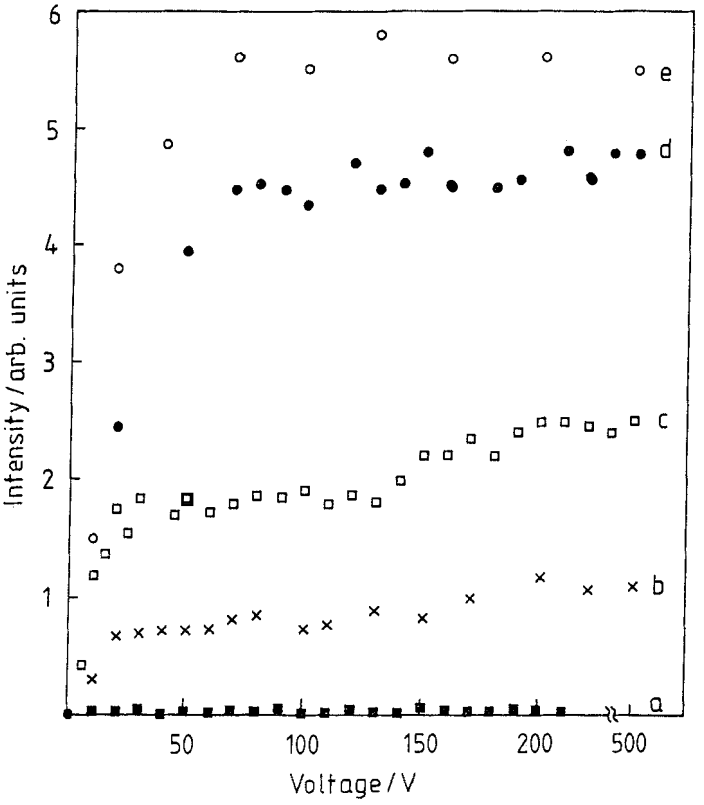

Figure 5. Electric field dependence of SHG intensity of compound **7** at various temperatures; $a = 135°C$, $b = 120°C$, $c = 105°C$, $d = 80°C$, and $e = 70°C$.

Downloaded At: 11:08 26 January 2011

phase, no significant SHG signal is observed up to 500 volts. This agrees with the small induced tilt angle of < 1 at these field strengths. However, in the S_C^* phase, the signal changes dramatically: above a low threshold voltage of about 10 volts, the SHG intensity exhibits a sudden jump and follows qualitatively the tilt angle behaviour shown in figure 4 (*a*). The SHG signal increases with decreasing temperature and becomes nearly independent of the applied electric field at low temperatures. The threshold voltage is due to the minimum voltage required for unwinding the S_C^* helix. The pitch of compound **7** is in the visible range at the upper end of the S_C^* phase.

The unique feature of this compound is the following: unwinding the helix at temperatures above the glass transition and then cooling the sample to room temperature results in a macroscopically uniform, dipolar oriented configuration which remains stable when the electric field is switched off. Even after four weeks of storage at room temperature, no observable change in the configuration occurred.

4.3. *Results for mixture* **7**/**8**

4.3.1. *Phase assignments*

As mentioned above, apart from investigating the single compound **7**, we also studied a 1 : 1 mixture of compounds **7** and **8** (mixture **7**/**8**). The aim was to improve

the aligning properties of our NLO material. Indeed, mixture **7/8** exhibits better alignment properties for planar orientation than compound **7**. The clearing temperature is reduced to 154°C. Below this temperature, a S_A phase occurs followed by a glass transition at 31°C. However, the S_A–S_C^* transition was not detected, either by polarization microscopy or by careful DSC measurements. But the switching properties of thin homogeneously aligned cells exhibit an anomalous behaviour that might be characterized by a mixed response, simultaneously showing S_A and S_C^* features. Studying the tilt angle and the switching current as a function of temperature and electric field, we found a combination of electroclinic and ferroelectric effects (see figure 4(*b*)). This type of behaviour has been reported by several research groups [13, 14], and has been denominated the soft mode ferroelectric effect [15]. It seems to occur in FLCs that possess strong lateral dipole moments and exhibit an anomalously strong electroclinic effect in the S_A phase. When such compounds are cooled towards the S_C^* phase, one finds an intermediate temperature range where the tilt angle is still strongly field dependent, while the graph of switching current versus voltage exhibits the characteristic peak due to the spontaneous polarization. A detailed discussion of this phenomenon is given in [15].

Our mixture 7/8 clearly exhibits the above mentioned features (figure 4*b*)). At 135°C, far above the S_C^* phase, we see a very strong electroclinic effect. When the temperature is lowered the tilt angle increases and deviates more and more from the linear field dependence. At the lowest temperature (23°C), the tilt angle reaches $\theta_t = 28°$ at $30\,V\,\mu m^{-1}$, but does not yet saturate.

The behaviour is also evident in the voltage dependence of the switching current and the corresponding optical transmission of the cell measured through crossed polarizers (see figure 6). But the interpretation of this behaviour is complicated. This is due to the high viscosity which leads to strong hysteresis effects in switching experiments at low temperatures.

The question of where to locate the S_A–S_C^* transition of mixture **7/8** at zero electric field is not easily answered. We made several attempts to elucidate the existence of a helical structure by studying the temperature dependence of the refractive indices (see §4.4.), of the birefringence, and by searching for the helical pitch. However, we could not find unambiguous experimental evidence for the pitch. Moreover, we obtained strong indications of a relaxation of the field induced tilted phase to an orthogonal, or at least close to orthogonal orientation at all temperatures down to 23°C. The detailed discussion of these complex findings will be reported separately. We conclude: if the helix formation occurs at all in mixture **7/8** above 23°C, then the cone angle under zero applied field is very small. One way to support this statement is to investigate the electric field dependence of the SHG signal. We measured this dependence using a 7 μm thick planar oriented cell (see figure 7). Clearly there is no indication of a threshold voltage and the SHG intensity increases almost linearly over a wide range of electric field strengths. Similar results were observed with homeotropic aligned cells.

4.4. *Refractive index and waveguiding properties of mixture* **7/8**

4.4.1. *Refractive index determination*

For the quantitative determination of NLO coefficients, the refractive indices, the optical anisotropy, and the dispersion must be known.

Due to the good aligning properties of mixture **7/8**, we were able to determine the above quantities with high precision. One approach was to prepare a homeotropically aligned, thin layer on the prism of an Abbé refractometer and to measure the

Downloaded At: 11:08 26 January 2011

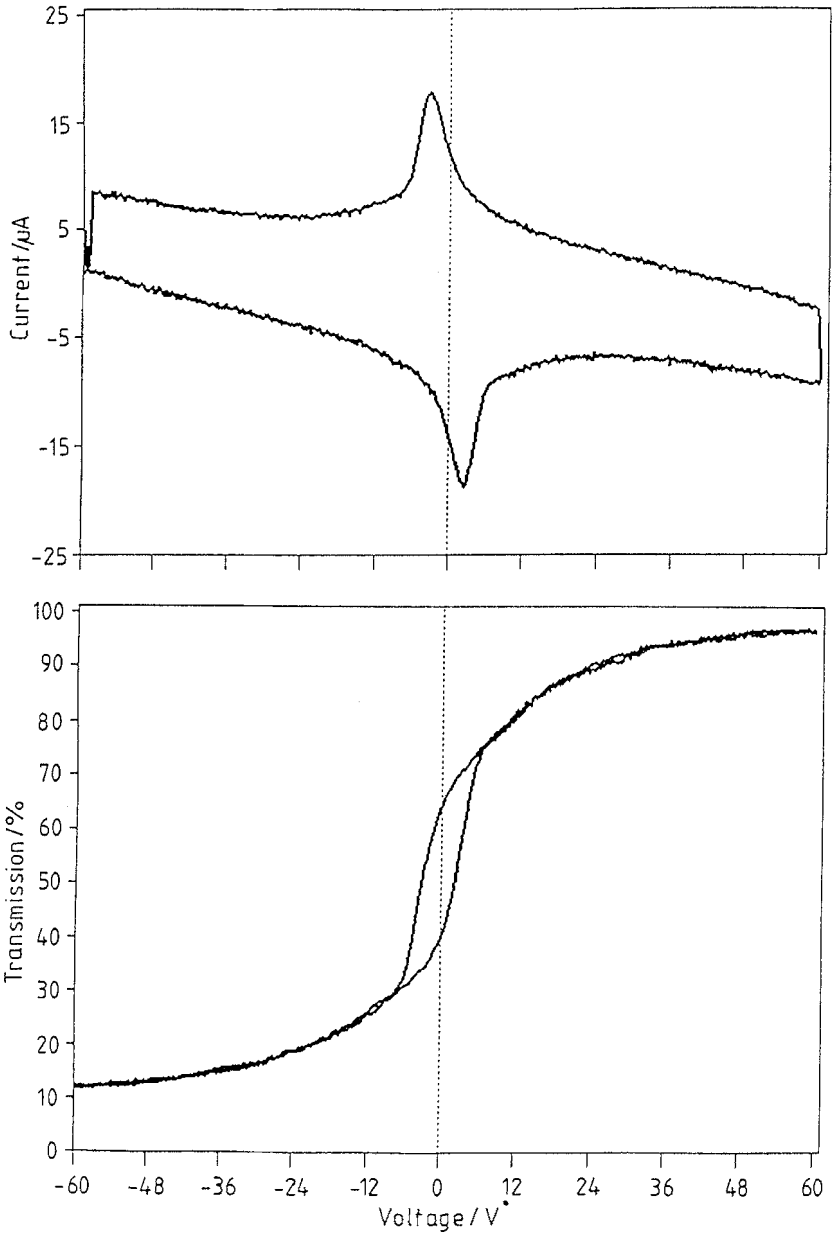

Figure 6. Upper part: switching current of mixture **7**/**8** at 66°C in a 6 μm thick, homogeneously aligned cell. Lower part: corresponding transmission of the cell through crossed polarizers.

temperature dependence of the indices with s and p polarized monochromatic light. The other approach was to determine the mode spectra of a homeotropically aligned slab waveguide at various laser wavelengths. Both attempts were successful, the results are shown in figures 1, 8 and 9. Moreover the mode spectra in figure 1 could be fitted exceptionally well assuming a uniaxial layer whose optical axis is oriented

Downloaded At: 11:08 26 January 2011

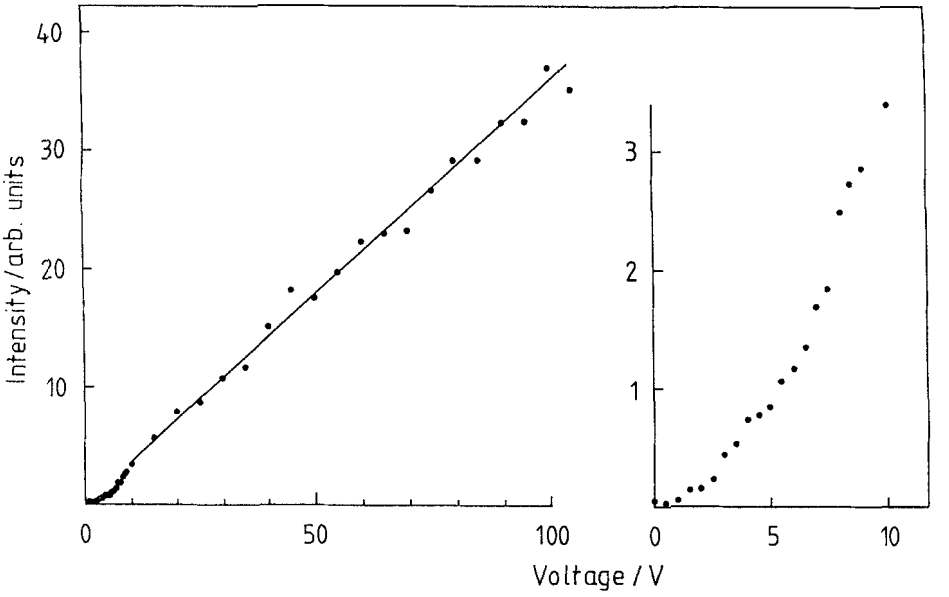

Figure 7. Electric field dependence of the SHG intensity of mixture **7**/**8** at 48°C in a 6 μm thick, homogeneous cell at oblique light incidence ($\theta_{in}=45°$).

Downloaded At: 11:08 26 January 2011

normal to the quartz surfaces. While the TE mode spectra determine the index parallel to the surface, the TM spectra determine the index normal to it. Analysing these spectra determined at $\lambda=488$ nm, 543 nm, 632 nm, and 1152 nm and fitting the data to the Sellmeier equation [16]

$$n^2(\lambda)-1=\frac{q}{\lambda_0^{-2}-\lambda^{-2}}+a \tag{1}$$

we obtained the index data, which are used below for a quantitative analysis of the SHG spectra.

4.4.2. *Waveguiding properties*

The damping constants of the guided modes were determined by measuring the intensity of the scattered light along the streak of the waveguide. Figure 10 shows the result for the most intense mode TM_5 which is $\approx 10\,dB\,cm^{-1}$. This value is not small, but it shows that waveguiding over several mm is possible. By further improving the alignment this value will certainly considerably improve too.

We have not yet made the same waveguiding experiments with compound **7**. Nevertheless it is safe to assume that the refractive indices of this compound are only slightly higher than those of mixture **7**/**8**. In particular, the dispersion, which is the sensitive parameter for phase matching and Maker fringe spectra is governed by the absorption of the NLO chromophore. Because of the identical chromophores, it seems justified to use the same data for compound **7** and mixture **7**/**8**; the excellent fit of the phase matching curve of compound **7** (see §4.5.) shows that this assumption is correct.

A different question is whether or not we can assume uniaxiality in our samples. One might expect that in the unwound helical state n_y is significantly larger than n_x

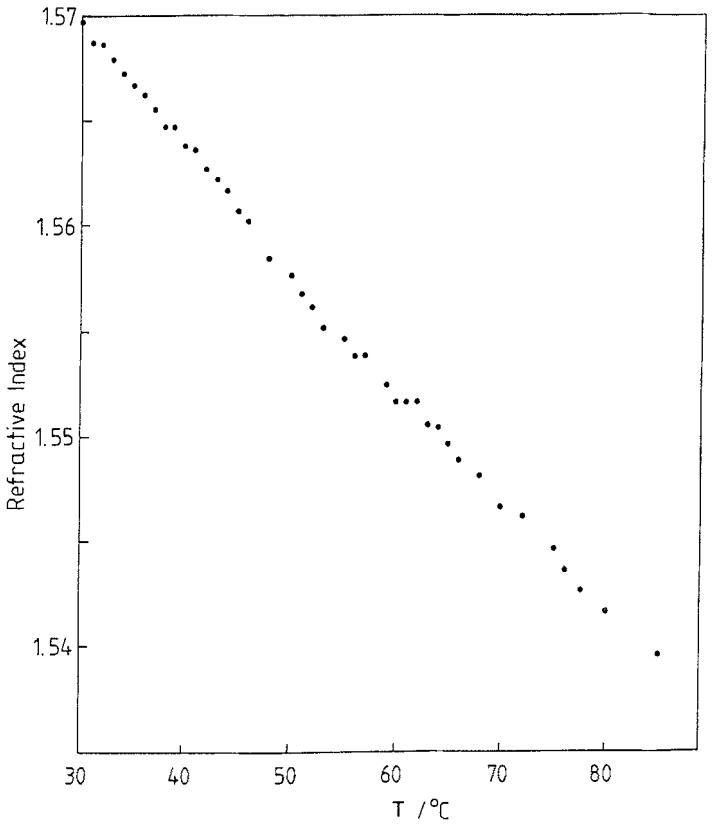

Figure 8. Temperature dependence of the ordinary refractive index of mixture **7**/**8**.

Downloaded At: 11:08 26 January 2011

(see figure 3). In the case of the nitro substituted biphenyl chromophore studied by Liu *et al.* [8], it was experimentally proven that these two indices are identical within experimental error. Until now we have not verified this aspect in our case. However, as long as n_x and n_y are not drastically different the values of the NLO coefficients reported below are not strongly affected.

In the following analysis of the SHG spectra of compound **7** and mixture **7**/**8**, we will use the following experimentally determined refractive index values:

$$n_x(\omega)=n_y(\omega)=1{\cdot}539,\ n_x(2\omega)=n_y(2\omega)=1{\cdot}576,\ n_z(\omega)=1{\cdot}65.$$

4.5. *Phase matching and determination of the NLO coefficients*

4.5.1. *Phase matching*

Since the optical anisotropy of our compounds is sufficiently large and positive, type I angular eeo phase matching [17] is expected to be observable. In this geometry (see figure 3) two extraordinary fundamental waves polarized in the plane of incidence generate an ordinary second harmonic wave polarized normal to this plane (parallel to the Y direction).

In the case of compound **7**, a 22 μm thick, homeotropically aligned cell with an electrode gap of 500 μm was used. The helix was unwound at 50°C by a DC electric field of 0·1 V μm^{-1}, and then cooled to 20°C. Then the field was switched off.

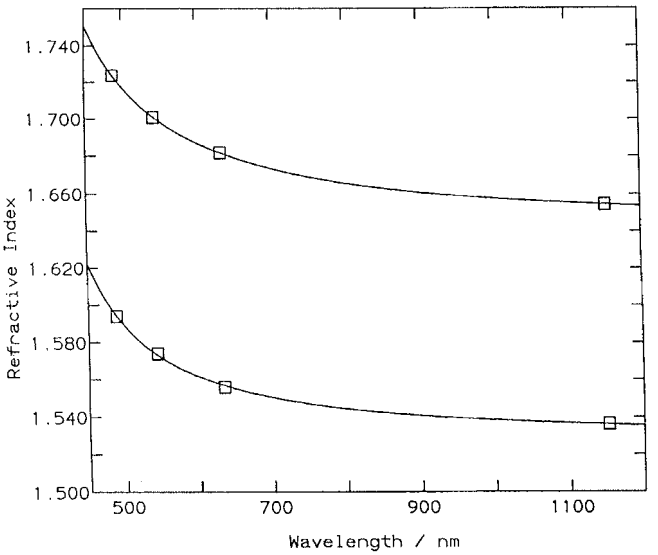

Figure 9. Refractive indices of mixture **7**/**8** determined by the mode spectra analysis of p polarized (TE modes, lower trace) and s polarized (TM modes, upper trace) incident light. The continuous curves are fitted to the Sellmeier equation.

Downloaded At: 11:08 26 January 2011

Figure 11 (*a*) shows the detected SHG intensity as a function of the angle of incidence. Using the above refractive index data, the phase matching angle can be calculated from [18]:

$$\Theta_m = \arctan\left[\frac{n_z(\omega)}{n_y(\omega)}\sqrt{\left(\frac{n_y(2\omega)^2 - n_y(\omega)^2}{n_z(\omega)^2 - n_y(2\omega)^2}\right)}\right]. \tag{2}$$

We find $\theta_m = 37°$, which is a fairly large value due to the large dispersion of compound **7**. Using the tilt angle $\theta_t = 23°$ determined at room temperature, we

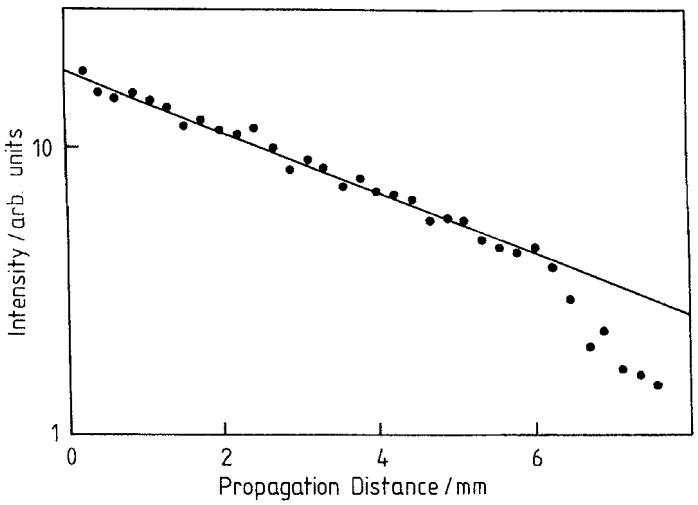

Figure 10. Determination of the damping factor for the mode TM_5.

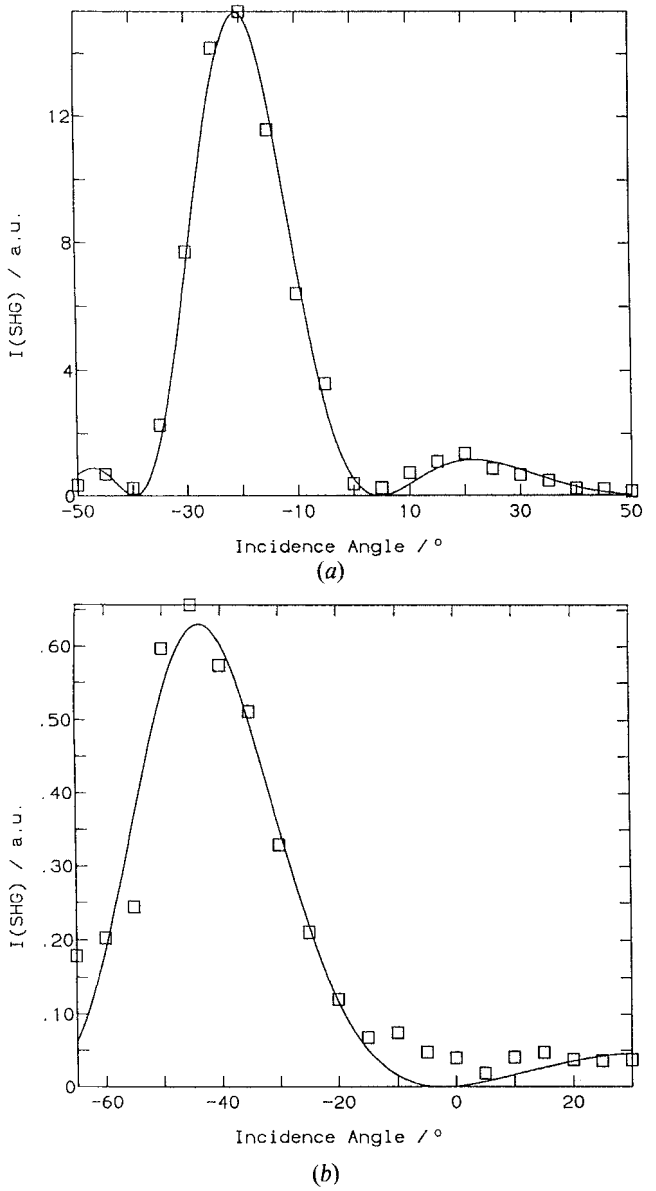

Figure 11. (*a*) and (*b*) Type I angular phase matching of (*a*) compound **7** and (*b*) mixture **7**/**8** as a function of incidence angle θ_{in}. The continuous curve is the best fit of equation (5) to the measured data.

recalculate the expected incidence angle θ_{in}(PM) for the phase matching condition. From this follows $|\theta_{in}(PM)| = 22{\cdot}7°$ which is in good agreement with $|\theta_{in}(PM)| = 21{\cdot}3°$ obtained directly from the phase matching curve (see figure 11 (*a*)).

The same experiment was performed for mixture **7**/**8**. Here a 15 μm thick cell was used with an electrode gap of 200 μm. Because the tilted orientation of this mixture is not stable at zero field strength, we applied an electric field of 5 V μm^{-1} at 23°C. As shown in figure 11 (*b*), the maximum of the phase matching curve occurs at

Downloaded At: 11:08 26 January 2011

$|\theta_{in}(PM)| = 43{\cdot}8°$ because the induced tilt angle is only about 10°. Again the measured and the estimated angles of incidence are in agreement.

4.5.2. *Determination of the NLO coefficients d_{ij}*

In the tilted, unwound helical state, the FLC layer is macroscopically homogeneous and has C_2 symmetry. The twofold axis of rotation is parallel to the Y direction (see figure 3), which is the direction of the spontaneous polarization. The tensor of the second order NLO coefficients d_{ij} is then given by [17]

$$d = \begin{pmatrix} 0 & 0 & 0 & d_{14} & 0 & d_{16} \\ d_{21} & d_{22} & d_{23} & 0 & d_{25} & 0 \\ 0 & 0 & 0 & d_{34} & 0 & d_{36} \end{pmatrix}. \tag{3}$$

Assuming that Kleinman degeneracy is valid [17] (the absorption maximum of our compounds is at 380 nm), the number of independent coefficients is reduced to four: $d_{14} = d_{25} = d_{36}$; $d_{23} = d_{34}$; $d_{21} = d_{16}$ and d_{22}. Depending on the polarizations used in the SHG experiments, these coefficients will show up separately or in characteristic combinations.

The coefficient d_{22} can be isolated by choosing s polarized fundamental waves which generate an s polarized second harmonic wave (ooo experiment). On the other hand the eeo phase matching experiment described above is determined by the angular dependent contributions of the three coefficients d_{14}, d_{23}, and d_{16}

$$d_{eff}(\theta) = d_{14}\sin(2\theta) + d_{23}\sin^2(\theta) + d_{16}\cos^2(\theta). \tag{4}$$

The angular dependence of the phase matching curve is given by [17, 19]

$$P^{2\omega} = \frac{2\omega^2 d_{eff}^2 L^2 (P^\omega)^2 (t^\omega)^4 T^{2\omega}}{\varepsilon_0 c^3 (n_e^\omega)^2 n_y^{2\omega} A} \frac{\sin^2(\Delta k L/2)}{(\Delta k L/2)^2}, \tag{5}$$

where $L = L_0/\cos(\theta_t - \theta)$ is the interaction length, $\Delta k = (4\pi/\lambda)(n_y^{2\omega} - n_e^\omega(\theta))$, where $n_e(\theta)$ is the effective index of the p polarized refracted fundamental beam, A is the beam area, t^ω and $T^{2\omega}$ are Fresnel transmission factors.

The absolute values of the NLO coefficients of equation (3) can then be determined by comparing the SHG intensity of the FLC samples with the SHG intensity of a crystalline quartz plate of known thickness using the known value of the d coefficient of quartz ($d_{11} = 0{\cdot}4\,\mathrm{pm\,V^{-1}}$ [19]).

4.5.3. *Determination of d_{22}*

Because the large SHG efficiency of our materials is sufficiently high, the easiest and probably most reliable way to determine d is to use cells which are thin compared with the coherence length l_c

$$l_c = \frac{\lambda_0}{4(n_y^{2\omega} - n_y^\omega)} \tag{6}$$

From the measured dispersion data follows $l_c = 7{\cdot}5\,\mu m$. Thus, $2\,\mu m$ thick cells were used to determine the SHG signal of compound **7** and mixture **7**/**8** at normal incidence. Comparison with the quartz standard gives the following values at 23°C:

$d_{22} = 5{\cdot}0\,\mathrm{pm\,V^{-1}}$ for compound **7** (zero field)

Downloaded At: 11:08 26 January 2011

and

$$d_{22} = 2{\cdot}1\,\text{pm V}^{-1} \text{ for mixture } \mathbf{7/8} \text{ (at a DC field of } 5\,\text{V}\,\mu\text{m}^{-1}).$$

4.5.4. *Determination of* d_{eff}

Analysing the phase matching curves described above, we determined the value of $d_{\text{eff}}(\theta)$ at the phase matching angle by comparison of the SHG intensity at the maximum of the phase matching curve with the quartz standard. The following effective NLO coefficients are found for our materials at room temperature:

$$d_{\text{eff}}(\theta_{\text{m}}) = 0{\cdot}78\,\text{pm V}^{-1} \text{ for compound } \mathbf{7}$$

and

$$d_{\text{eff}}(\theta_{\text{m}}) = 0{\cdot}68\,\text{pm V}^{-1} \text{ for the mixture } \mathbf{7/8} \text{ (at a DC field of } 5\,\text{V}\,\mu\text{m}^{-1}).$$

The uncertainty of all coefficients is of the order of 15 per cent.

4.6 *Computer simulation*

Analogously to [8], we finally determined the coefficients d_{14}, d_{16} and d_{23} by fitting the theoretically expected phase matching curve (see equation (5)) to the measured data. All three coefficients contribute to d_{eff} (see equation (4)). Figure 11 (*a*) shows this fit for compound **7**. We obtain

$$d_{14} = 0{\cdot}49\,\text{pm V}^{-1}, \quad d_{16} = 1{\cdot}13\,\text{pm V}^{-1}, \quad d_{23} = 1{\cdot}46\,\text{pm V}^{-1}.$$

We now add a few remarks concerning the parameters in our computer simulation. The refractive index data used in our fit were independently determined. However, since our samples could not be made thicker than 20 μm, it was necessary to determine the angular dependence of the SHG signal over a large angular range in order to reveal the interference structure. The consequence is that the angular dependences of all parameters involved had to be seriously taken into account. This applies especially to the Fresnel factors, but also to the angular dependent refractive index seen by the refracted fundamental beam which depends on the tilt angle and on n_x and n_z [8]. Also d_{eff} is strongly angular dependent, varying by a factor of 2 over the measured angular range. Therefore the fitted coefficients are by no means arbitrary. None the less, it is difficult to estimate the precision of these values.

The calculated curve shown in figure 11 (*b*) is also fitted with respect to d_{23}, d_{14} and d_{16}. The inferior quality of the experimental data prohibits reliable fitting results for the individual coefficients.

5. Conclusion

We have synthesized 3- and 4-ring compounds with 4-nitroaniline NLO chromophores which exhibit FLC phases and show the strongest second order NLO responses reported thus far. Large values for all relevant non-linear optical coefficients are determined which compare favourably with state of the art inorganic NLO crystals like $LiNbO_3$.

Angular phase matching is demonstrated as is waveguiding in homeotropically aligned layers. The combination of large NLO coefficients, stable operability at room temperature, phase matching, and waveguiding may render the new NLO-FLC materials applicable in integrated optics waveguide devices.

Downloaded At: 11:08 26 January 2011

The existence of a glass transition above room temperature allows us to freeze the NLO active configuration in the S_C^* phase by cooling the materials below T_g, while applying an electric field. Removing the electric field below T_g does not cause the NLO activity to decay.

References

[1] BARKNIK, M. I., BLINOV, L. M., and SHTYKOV, N. M., 1984, *Zh. eksp. teor. Fiz.*, **86,** 1681.
[2] VTYURIN, A. N., ERMAKOV, V. P., OSTROVSKII, B. I., and SHABANOV, V. F., 1981, *Kristallografiya*, **26,** 546.
[3] BLINOV, L. M., BAIKALOV, V. A., BARNIK, M. I., BERESNEV, L. A., POZHIDAYEV, E. P., and YABLONSKY, S. V., 1987, *Liq. Crystals*, **2,** 121.
[4] LIU, J. Y., ROBINSON, M. G., JOHNSON, K. M., and DOROSKI, D., 1990, *Optics Lett.*, **15,** 267.
[5] TAGUCHI, A., OUCJI, Y., TAKEZOE, H., and FUKUDA, A., 1989, *Jap. J. appl. Phys.*, **28,** 997.
[6] WALBA, D. M., and ROS, M. B., 1991, *Molec. Crystals liq. Crystals*, **198,** 51.
[7] KAPITZA, H., ZENTEL, H., TWIEG, R. J., NGUYEN, C., VALLERIEN, S. U., KREMER, F., and WILSON, C. G., 1990, *Adv. Mater.*, **11,** 539.
[8] LIU, J. Y., ROBINSON, M. G., JOHNSON, K. M., WALBA, D. M., ROS, M. B., CLARK, N. A., SHAO, R., and DOROSKI, D., 1991, *J. appl. Phys.*, **70,** 3426.
[9] NICOUD, J. F., and TWIEG, R. J., 1987, *Nonlinear Optical Properties of Organic Molecules and Crystals*, edited by D. S. Chemla and J. Zyss (Academic Press), p. 227.
[10] WALBA, D. M., and CLARK, N. A., 1988, *Ferroelectrics*, **84,** 65.
[11] TAGUCHI, A., OUCHI, Y., TAKEZOE, H., and FUKUDA, A., 1989, *Jap. J. appl. Phys.*, **28,** L 997.
[12] UTSUMI, M., GOTOU, T., DAIDO, K., OZAKI, M., and YOSHINO, K., 1991, *Jap. J. appl. Phys.*, **30,** 2369.
[13] YANG, Y. B., MOCHIZUKI, A., NAKAMURA, N., and KOBAYASHI, S., 1991, *Jap. J. appl. Phys.*, **30,** L 612.
[14] ABDULHALIM, I., and MODDEL, G., 1991, *Liq. Crystals*, **9,** 493.
[15] ANDERSSON, G., KUCYNSKI, W., LAGERWALL, S. T., SKARP, K., and STEBLER, B., 1988, *Ferroelectrics*, **84,** 285.
[16] BORN, M., and WOLF, E., 1980, *Principles of Optics* (Pergamon Press), 6th edition, p. 94.
[17] ZERNIKE, F., and MIDWINTER, J. E., 1973, *Applied Nonlinear Optics* (Wiley), p. 54.
[18] OZAKI, M., MIMOTO, K., and YOSHINO, K., 1989, *Tech. Rep. Osaka Univ.*, **39,** 217.
[19] JERPHAGNON, J., and KURTZ, S. K., 1970, *J. appl. Phys.*, **41,** 1667.

Downloaded At: 11:08 26 January 2011